J. Phys.: Condens. Matter **20** (2008) 494237 (10pp) doi:10.1088/0953-8984/20/49/494237

Interfaces in confined Ising models: Kawasaki, Glauber and sheared dynamics

Thomas H R Smith[1], Oleg Vasilyev[2,3], Douglas B Abraham[4], Anna Maciołek[2,3,5] and Matthias Schmidt[1,6]

[1] H H Wills Physics Laboratory, University of Bristol, Tyndall Avenue, Bristol BS8 1TL, UK
[2] Max-Planck-Institut für Metallforschung, Heisenbergstraße 3, D-70569 Stuttgart, Germany
[3] Institut für Theoretische und Angewandte Physik, Universität Stuttgart, Pfaffenwaldring 57, D-70569 Stuttgart, Germany
[4] Theoretical Physics, Department of Physics, University of Oxford, 1 Keble Road, Oxford OX1 3NP, UK
[5] Institute of Physical Chemistry, Polish Academy of Sciences, Department III, Kasprzaka 44/52, PL-01-224 Warsaw, Poland
[6] Theoretische Physik II, Universität Bayreuth, Universitätsstraße 30, D-95440 Bayreuth, Germany

Received 31 July 2008, in final form 1 October 2008
Published 12 November 2008
Online at stacks.iop.org/JPhysCM/20/494237

Abstract

We study interfacial properties of the phase-separated two-dimensional Ising model. The interface between coexisting phases is stabilized by two parallel walls with opposing surface fields. A driving field parallel to the walls is applied which (i) either acts locally at the walls or (ii) varies linearly with distance across the strip. Using computer simulations with Kawasaki dynamics, we found (Smith *et al* 2008 *Phys. Rev. Lett.* **101** 067203) that the system reaches a steady state with a sharper magnetization profile, reduced interfacial width, and faster decay of correlations along the interface, as compared to the equilibrium case. Here we present new results for the bond energy profile, providing further evidence for the picture wherein shear acts as effective confinement in this system. As a prerequisite for understanding the driven system, we investigate the pronounced differences between Kawasaki (spin-exchange) and Glauber (spin-flip) dynamics in the confined equilibrium system.

(Some figures in this article are in colour only in the electronic version)

1. Introduction

As much as studying the Ising model in equilibrium has helped to gain insights into critical phenomena and the structure and thermodynamics of interfaces, *kinetic* Ising (or lattice gas) models have contributed greatly to the emerging understanding of dynamic phenomena in condensed matter. Examples include dynamic critical phenomena [1], kinetics of phase separation, i.e., nucleation and domain growth [2], dynamics of fluid spreading and wetting [3], and the glass transition [4].

In these simple models the time evolution proceeds according to given stochastic rules. One assumes that the (Ising) spins are in contact with a heat bath at temperature T which induces random transitions of spin states. The heat bath is accounted for indirectly via transition probabilities for elementary moves; these completely specify the dynamics. Often the transition probabilities are taken to not depend on the history of the system, so that the stochastic process is Markovian. Also, they are suitably constructed to reproduce the equilibrium state, i.e., such that the condition of detailed balance for the Gibbs probability distribution is satisfied. Underlying the entire scheme is the idea of coarse graining [5]. A record of the dynamical state is only kept at discrete time and space points. The lattice gas 'particles' can be thought of as fluid elements; the positions and momenta of the constituent atoms are not followed.

Typically two different types of the elementary spin transitions are considered. In the so-called spin-flip dynamics originally proposed by Glauber [6], the simplest move is a random flip of only one spin at a given time, so that both the total magnetization and the total energy of the system may have changed after the transition. These single spin-flip dynamics cannot describe transport phenomena such as diffusion or heat conduction, where the quantities of interest

are conserved. In these situations Kawasaki dynamics [7] are more appropriate, in which the simplest transition induced by the heat bath is an exchange of two nearest-neighbour spins, so that the total magnetization of the system is conserved locally (and hence globally). In the equivalent lattice gas formulation one considers particles located on a lattice on which they move and interact. The single-spin flip corresponds to the spontaneous appearance/disappearance of a particle, which is somewhat artificial in this context. The spin-exchange transition corresponds to the physically more plausible jump of the particle to a neighbouring (empty) site.

An important generalization of the kinetic Ising lattice gas model is that to systems driven out of equilibrium by external force fields. Such models are referred to as driven lattice gas models or driven diffusive systems [8, 9]. Driving induces preferential hopping of the particles in the local direction of the external driving force field—jump rates are biased in that direction and suppressed in the opposite direction, breaking the spatial symmetry; these rates usually obey a 'local detailed balance'. The resulting steady states are no longer equilibrium states for any Hamiltonian and are characterized by a steady particle current. A well studied example is the nearest-neighbour interacting lattice gas driven by a spatially uniform and temporally constant external force field, known as the Katz–Lebowitz–Spohn (KLS) model [10]. Stationary properties, in particular the out-of-equilibrium phase diagram and critical behaviour of this model, have been investigated in great detail [8, 11] using several approaches, ranging from Monte Carlo simulations to field-theoretical methods.

Studying Ising models has greatly increased our understanding of interfacial phenomena [12, 13]. Through the equivalence to the lattice gas model the obtained results are pertinent to fluid interfaces—spin variables, which take values ± 1, map on to particle occupation numbers 1 and 0 for a site. The magnetization profile, for example, is then equivalent to a lattice gas density profile. In the case of sub-critical Ising ferromagnets, phase coexistence is between two phases of opposite magnetizations; for a simple fluid below its critical point between liquid and gas, while for a binary liquids mixture below its consolute point it is between liquids of differing composition. Rigorous exact results for Ising interfaces have supported the evidence from phenomenological and approximate theories that interfacial properties depend crucially both on dimensionality and on geometry of the system, and that in equilibrium the interface between suitably organized coexisting phases exhibits large spatial fluctuations. These interfacial fluctuations occur on a scale determined by a macroscopic length rather than the bulk correlation length, as classical (mean-field) theories, such as van der Waals theory, would suggest [14, 15], and diverge in the thermodynamic limit (unless a suitable external field such as gravity is applied).

For instance, if an interface in the two-dimensional (2d) Ising lattice gas model is pinned at two points separated by a geodesic distance L, then its rms width, as revealed by the local magnetization [16], diverges as $\sqrt{L}$ for $0 < T < T_c$, where T is the temperature, T_c is its critical value and $T_R = 0$ is the roughening temperature in this case. This result agrees with the phenomenological capillary wave theory [17, 18], which indicates that the location (height) of the interface $h(x)$ with mean orientation $(1, 0)$ as a function of position $(x, 0)$ satisfies

$$C(x) \equiv \langle h(0)h(x)\rangle = \frac{k_B T}{\Gamma}\int \frac{e^{iqx}}{\xi_\parallel^{-2} + q^2}\,dq, \qquad (1)$$

where k_B is the Boltzmann constant, Γ is the interfacial stiffness, and $\xi_\parallel$ is the lateral correlation length (along the interface). In the absence of a gravitational field the decay of height–height correlations is determined by a low wavenumber ('infrared') cutoff $q_0 \propto L^{-1}$ in the integral (1). A measure of the interfacial width is the mean-square displacement of the interface,

$$w^2 = \langle h(0)^2\rangle \sim \frac{k_B T}{\Gamma}\frac{(d-1)}{(3-d)}\left[\left(\frac{L}{a}\right)^{3-d} - 1\right] \qquad (2)$$

where a is a microscopic length scale. Thus in $d = 2$, $w^2 \approx Lk_BT/\Gamma$, in agreement with exact results.

Much can be learnt from the problem of the interface confined between two walls with finite separation L_y. For the 2d Ising lattice gas model the magnetization profile $m_{eq}(y)$ has been obtained for any given finite strip width L_y as a determinant, which is then evaluated numerically [19] (further analytic progress would be valuable). The numerical results indicate that the interface sweeps out essentially the entire width of the strip, such that its width $w \sim L_y$, although it will experience entropic repulsion at its extremities. Here, w is the characteristic length of the one-point function setting up the length scale in the y direction. As a result the soft-mode part of the magnetization profile obeys the scaling relation

$$\frac{m_{eq}(y, T, L_y)}{m_b(T)} = \tilde{\mathcal{M}}_{eq}(y/w) = \mathcal{M}_{eq}(y/L_y), \qquad (3)$$

where $m_b(T)$ is the spontaneous bulk magnetization and $\tilde{\mathcal{M}}_{eq}$, $\mathcal{M}_{eq}$ are scaling functions. The scaling form with w (first equality in (3)) is often used in the context of fluid interfaces. The interface itself acts as a trap for mobile lattice gas 'particles', but there exists a transport mode with relatively low activation energy along the interface itself [20].

Although no rigorous proof is available, the three-dimensional (3d) Ising model is assumed to also have a rough phase for $T_R < T < T_c^{3d}$ (in 3d, $T_R > 0$), but the mechanism by which it could be established is completely different. The interface configurations which result in interference with the boundary are needle-like, with high acicularity [21]; this restricts transport much less than meandering. Finally we note that for the case of the interface confined between two walls the standard capillary wave model does not apply; it has to be extended to take into account entropic repulsion from the walls.

As mentioned above, the critical and bulk properties of the driven lattice gas (KLS [10]) have been studied in detail. The interface between coexisting phases has also been studied, mostly by simulation [22–24], but also by theoretical approaches [25]. Leung *et al* [23] studied the interface of the two-dimensional KLS model in the sub-critical regime via Monte Carlo simulations. The total magnetization was fixed at zero, corresponding to half-filling in lattice gas language. The

lattice dimension L_y normal to the interface (and the walls) was chosen to be large enough for repulsion between the interface (oriented along x) and the walls to be unimportant. Simulations were done using a generalization of the local spin-exchange Kawasaki dynamics [7] mentioned above; see section 2 for a definition of the transition rates in the driven case. Leung *et al* noted that owing to the *local* particle number conservation, the evolution of a system with an interface under these dynamics is extremely slow, since particles must be transported 'step-by-step' in order to change the configuration of the interface. We investigate the differences between Kawasaki and spin-flip (Glauber) dynamics later in this paper.

In [23] the magnetization profile $m(y)$ was found to become much sharper upon increasing the applied drive: $|m(y)|$ stayed close to unity much further away from the walls as compared to the equilibrium profile, and thus changed sign much more sharply. This indicates that the interface is less rough when drive is applied; capillary-wave-like fluctuations are suppressed. Leung *et al* also investigated the spatial and temporal correlations of the interfacial height (where the height was defined by a coarse-graining method), and the finite-size scaling of the interfacial width (expected to scale as $w \sim \sqrt{L_x}$ in this case, see equation (2)). From the behaviour of the latter quantity, they speculated that the interface would in fact be *smooth* in the thermodynamic limit—i.e., the width would tend to a finite value as the system size is increased. This is a striking example of the differences between equilibrium and non-equilibrium systems—recall from the above discussion that, in equilibrium, the width diverges in the thermodynamic limit. A subsequent study [24] of the Fourier transform of the height correlation function, $C(q)$, showed $C(q) \sim 1/q^{0.67}$, markedly different from the $1/q^2$ equilibrium (capillary wave—see equation (1)) behaviour above the roughening transition. The behaviour in the driven case is consistent with a smooth interface, since the squared interfacial width is proportional to $\int C(q)\,\mathrm{d}q$ with suitable wavenumber cutoffs limiting the range of integration. In the same study the previously predicted $1/q$ decay of $C(q)$ [25] (via a coarse-grained, Langevin equation approach) for the *randomly* driven KLS model was observed.

Further motivation for studying driven interfaces comes from experiment. Colloidal dispersions form convenient systems in the study of interfaces, both in and out of equilibrium. A recent example of a non-equilibrium study may be found in [26], where the sheared interface of a demixed colloid–polymer system was investigated using real-space (confocal microscopy) techniques. Real-space visualization of interfacial fluctuations is possible due to the low interfacial tension in such a system, leading to large interfacial roughness and slow spatial and temporal decay of fluctuations [27]. Colloid–polymer mixtures can be subject to shear in well-controlled ways [28, 29]. In [26], the authors found a reduced interfacial roughness when shear was applied, both visually and in results for the width and correlation function of the height of the interface. The results were analysed in the context of (equilibrium) capillary wave theory [18, 30]; using this approach, Derks *et al* concluded that the correlation length along the interface was increased, and that an *effective* surface tension was higher than in the equilibrium system.

Motivated by a need to understand fluid interfaces in relevant out-of-equilibrium situations, such as under the influence of shear flow, we have studied fluctuating interfaces in driven Ising lattice gas models. To this end, we have studied a sheared 2d Ising lattice gas in strip geometry, with two variants of the driving field, which form analogues of shearing in a real liquid. The geometry considered, with the lattice dimension L_x along the interface much greater than the size L_y normal to it, is very different from that of Leung *et al*—for example, in equilibrium $w \sim L_y$ in strip geometry. An advantage of this choice of geometry is the availability of exact results and known scaling forms in equilibrium (see above). Results for several quantities of interest, namely the particle current, magnetization profile, and two-body correlation functions of the interface have been reported in [31], where by rescaling the driven results, we could interpret the effect of shear as an effective increase of confinement of an equilibrium system. Here, we present new results which further support the effective confinement picture.

We believe that studying lattice models complements previous work on continuum models, such as using molecular dynamics techniques applied to liquid–liquid [32, 33] and nematic–isotropic [34] interfaces. Note that there are important differences between lattice models with stochastic dynamics and continuum fluid dynamics, in particular due to that fact that the former lack a description of inertia. For static interfacial properties in equilibrium however, the results for the Ising model should be representative of its universality class. As such, leaving the issue of dimensionality aside, the results are expected to describe real liquid interfaces.

Driven Ising models have proved valuable in studying dynamical transitions of the driven interface [35], the kinetics of domain growth [36], and nucleation under shear [37]. In [36, 37], non-conserving (spin-flip) dynamics were used, and the shear introduced as a separate step in the simulation algorithm. Shearing a fluid is an important example of a system driven away from equilibrium. It affects the liquid structure [38] and can cause new phase transitions [39]. Shear was also studied in hard core lattice models [40].

We also explore the differences in the results for one-and two-body functions obtained by Monte Carlo simulations with spin-flip (Glauber) and spin-exchange (Kawasaki) dynamics. As we demonstrate, for a finite system in *equilibrium*, these can be quite striking. The different types of dynamics sample different statistical ensembles. Glauber dynamics generates microstates of an ensemble where the total magnetization can fluctuate (at vanishing bulk magnetic field in our case). In lattice gas language, this corresponds to a grand ensemble where the chemical potential is fixed, such that on average the system is half-filled. Kawasaki dynamics sample an ensemble with fixed total magnetization, corresponding to a canonical ensemble with fixed total number of particles. As we investigate in detail below, this difference has a profound influence on the interfacial properties of confined finite systems, as the total (vanishing) magnetization in the Kawasaki case restricts the mean interfacial position at the centre of the system more strongly than is the case for Glauber dynamics. Unfreezing this 'zero mode' in Glauber dynamics

leads to pronounced finite-size difference both in one- and two-body correlation functions.

It is well known that different dynamics yield different paths and rates of approach to equilibrium [41]; indeed cluster algorithms take advantage of this fact to speed up Monte Carlo simulation of many models significantly. The differences between dynamics (both non-conservative) whose transition rates factorize into a spin interaction part and an external field part, and those which do not ('soft' and 'hard' dynamics, respectively), have been studied in the context of field-driven solid-on-solid (SOS) and Ising interfaces [42, 43]. Rikvold and Kolesik found the intrinsic SOS interface width to be independent of applied (Hamiltonian) field for soft dynamics, in contrast with the hard case, where this quantity grows with increasing field. Good agreement between their analytic results and simulation was found. Our comparison is between conservative and non-conservative dynamics, both in the absence of a Hamiltonian external field. This is an interesting problem, because spin-flip dynamics are typically used in static studies, but as explained above, for our purposes Kawasaki dynamics are a more natural choice—thus it is worthwhile to compare the two dynamics in the (simpler) equilibrium context.

The remainder of this paper is organized as follows. In section 2 we define the sheared Ising lattice gas model. We describe new results for the energy bond profile in section 3.1. In section 3.2 we present a comparison of Glauber and Kawasaki dynamics for confined systems in equilibrium. We conclude and mention some future avenues of research in section 4.

2. Sheared Ising model and simulation methods

The 2d sheared Ising lattice gas amounts to a generalization of a confined KLS [10] model to spatially non-uniform drive. In spin language, the Hamiltonian H is of the ferromagnetic Ising nearest-neighbour type: $H = -J\sum_{\langle i,j\rangle}\sigma_i\sigma_j$, where $\langle i, j\rangle$ indicates a sum over nearest-neighbour sites i and j; $J > 0$ is the spin–spin coupling constant, and the spins take on values $\sigma_i = \pm 1$, corresponding to particle occupation numbers $\tau_i = (\sigma_i + 1)/2 = 0, 1$.

We consider a 2d square lattice of dimensions $L_x \times L_y$, with $L_x \gg L_y$, so that in equilibrium scaling of the type (3) is expected to hold, and the interfacial width $w \sim L_y$. The interface is induced by means of two walls of fixed spins: $\sigma_i = +1$ at the top ($y = L_y + 1$) and $\sigma_i = -1$ at the bottom ($y = 0$) edges of the lattice. These boundary conditions strongly energetically favour up and down (respectively) spin regions in their vicinity; this causes the interface to be oriented along the x direction. Periodic boundary conditions are applied at the x edges of the lattice. See figure 1(a) for an illustration of the system.

In order to introduce drive, the equilibrium Kawasaki dynamics are supplemented by a force field $JF(y)$ oriented parallel to the x direction. We consider two forms for $F(y)$. In model I, only particles in the layer adjacent to each wall are

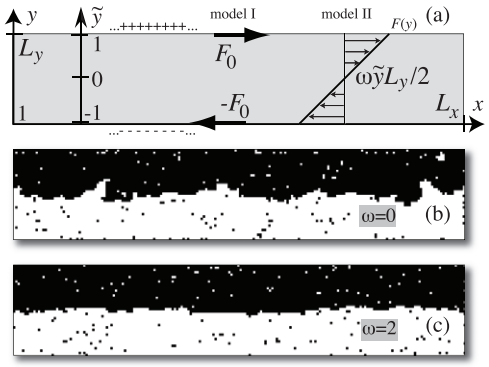

Figure 1. (a) Illustration of a 2d Ising strip confined between $+/-$ walls and under the influence of a driving field $F(y)$ along the x-direction. Models I and II discussed in the text are shown: in model I, the drive acts only at the walls, while in model II $F(y)$ varies linearly with y through the system. (b) Snapshot from simulation with $T/T_c = 0.75$, $L_x = 200$, and $L_y = 20$ at equilibrium; black (white) regions indicate $\sigma_i = +1(-1)$. (c) Same as (b) but under strong shear-like drive according to model II with $\omega = 2$.

driven, in opposite directions at the top and bottom walls:

$$F(y) = \begin{cases} F_0 & y = L_y, \\ -F_0 & y = 1, \\ 0 & \text{otherwise.} \end{cases} \qquad \text{(model I)} \qquad (4)$$

In the limit $F_0 \to \infty$ these driven layers form totally asymmetric exclusion processes [8], coupled to an Ising strip (which of course contains both bulk-like and interfacial thermal fluctuations; the solution requires advanced transfer-matrix approaches [19]). In model II, the field varies linearly with y across the strip, and is zero at the mean interface position in the centre (see figure 1)—due to the finite lattice spacing this point lies *between* two rows if L_y is even, as it always is taken to be. The functional form is thus

$$F(y) = \omega\left[y - (L_y + 1)/2\right], \qquad \text{(model II)} \qquad (5)$$

where ω is the dimensionless change in field between two rows; in the continuum limit we would have $\omega = \partial F/\partial y$. One can also define a scaled and shifted variable $\tilde{y} = (2y - L_y - 1)/L_y$, which is zero in the centre of the strip and whose range is independent of L_y; then $F(y) = \omega\tilde{y}L_y/2$ for model II. This model can be thought of as mimicking the effects caused by the flow of a background solvent [26].

In both models, the field acts to modify the Kawasaki exchange rates (which are of Metropolis type), so that the non-equilibrium rates are $\min\{1, \exp(-(\Delta H + \Delta F)/(k_B T))\}$. Here, ΔH is the usual change in internal energy incurred by the proposed exchange, calculated from the Hamiltonian, and k_B is the Boltzmann constant. ΔF is the work done by or against the force field—it takes values $-JF(y), +JF(y)$, and 0, for the cases where the exchange would cause the spin species corresponding to a particle to move with, against, and perpendicular to the field, respectively. Thus moves in the y direction are unaffected and occur with normal equilibrium rates, but moves along x are enhanced or suppressed. Detailed

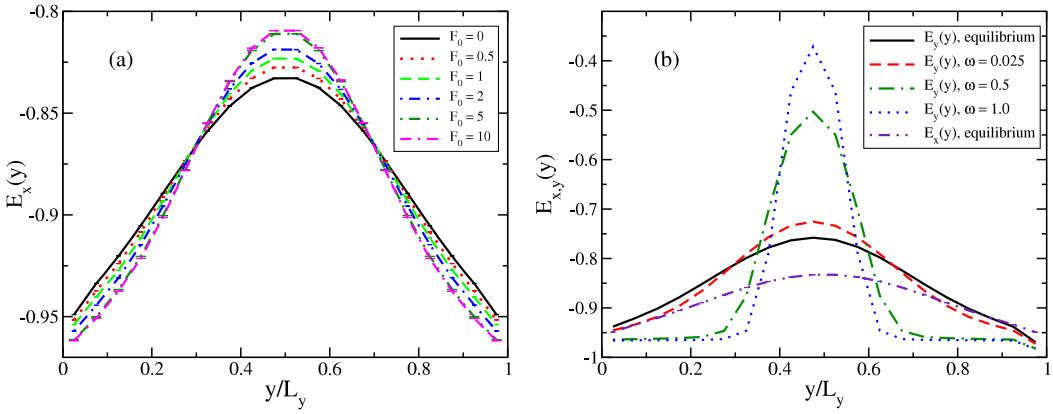

Figure 2. Energy bond profiles $E_x(y)$ and $E_y(y)$ as a function of scaled coordinate y/L_y, for a $T = 0.75T_c$, $L_x = 200$, $L_y = 20$ system. (a) Model I: results for $E_x(y)$ (only) with a variety of boundary drive strengths F_0, as well as the equilibrium result with Kawasaki dynamics. (b) Results for $E_x(y)$ and $E_y(y)$ in equilibrium, and for $E_y(y)$ with small and large field gradient ω in model II.

balance is violated, and the system is out of equilibrium. These dynamics capture the local conservation of particle number and the competition of forced transport with diffusive motion.

We have carried out extensive Monte Carlo (MC) simulations of the above models, as well as of the equilibrium case ($\omega = 0$, $F_0 = 0$) using single-spin and multi-spin [41, 44] coding techniques. The multi-spin technique allows simulation of 64 independent systems at once on a 64-bit computer system, by taking advantage of bitwise operations that can be carried out efficiently on a set of bits. Briefly, each site in the lattice is represented by a 64-bit variable, each of whose each bits corresponds to a different system. In each MC step, one constructs variables which specify how many anti-aligned neighbours each exchangee has, and creates random bit patterns so that the exchange is carried out with the appropriate probability. These variables are then combined with the appropriate bitwise operations to determine whether or not to carry out the exchange. We have extended the multispin algorithm for Kawasaki dynamics [44] to include drive; in this way we obtain much improved statistics over the single-spin case for a given amount of computer time. Multi-spin and single-spin results are consistent to within the error bars of the single-spin data. Figures 1(b) and (c) show snapshots of simulation configurations, in equilibrium and under drive in model II.

As discussed above in the context of the uniformly driven lattice gas, the relaxation of a system with an interface under Kawasaki dynamics is very slow, leading to both a long initial transient time to reach a steady state, and long correlation times once in that steady state. Thus run lengths of the order of $N_{MC} = 10^8$ MC sweeps ($L_x \times L_y$ trial moves form one MC sweep) are required. We find that applying drive in fact improves the situation, due to the increased rate of transport in the system.

3. Results

3.1. Bond energy profiles under shear

Here we present new results to complement those in [31]. The between-row bond energy profile $JE_y(y)$ is defined as the average bond energy between a spin in row y and its neighbour in row $y + 1$ via:

$$E_y(y) = -\left\langle \frac{1}{L_x} \sum_{x=1}^{L_x} \sigma(x, y)\sigma(x, y+1) \right\rangle. \qquad (6)$$

The in-row energy profile $JE_x(y)$ is similar, but measures interactions between spins in the *same* row:

$$E_x(y) = -\left\langle \frac{1}{L_x} \sum_{x=1}^{L_x} \sigma(x, y)\sigma(x+1, y) \right\rangle. \qquad (7)$$

Thus negative values of $E_x(y)$ and $E_y(y)$ close to the minimum of -1 imply that almost all bonds are between like spins, so that the system is locally strongly ordered. We first discuss the common features of $E_x(y)$ and $E_y(y)$—in the following, $E(y)$ represents both functions. We expect $E(y) \approx -1$ near the (fixed spin) walls; this is indeed confirmed in figure 2, which displays results both for models I and II. For both equilibrium and driven cases, near the centre of the system, $|E(y)|$ is smaller than at the boundaries, reflecting the presence of the interface in this region. When boundary drive (model I) is applied, $|E(y)|$ is increased near the walls, as compared to the equilibrium case. This indicates an increase in order near the walls, consistent with results for the magnetization profile [31]. The strength of the effect increases with larger values of F_0, up to the saturation value of $F_0 \approx 5$, beyond which further changes are very small (the saturation is due to the field appearing in the exponential in the transition rates—see section 2). We believe this effect is due to the boundary drive breaking up clusters of the 'wrong' spin species near a wall, which otherwise, in the absence of drive, would be relatively long-lived. Once such clusters are broken up, individual spins may diffuse freely in the bulk until they find the interface, and thus 'their own' phase again. This process leads to increased magnetization near the walls, and therefore an increase in $|E(y)|$. In model II, the same trend is observed when drive is applied; for (weak) $\omega = 0.025$ the size of the effect is similar to strong boundary drive. Upon increasing ω the effect becomes much larger; the profile is almost flat from

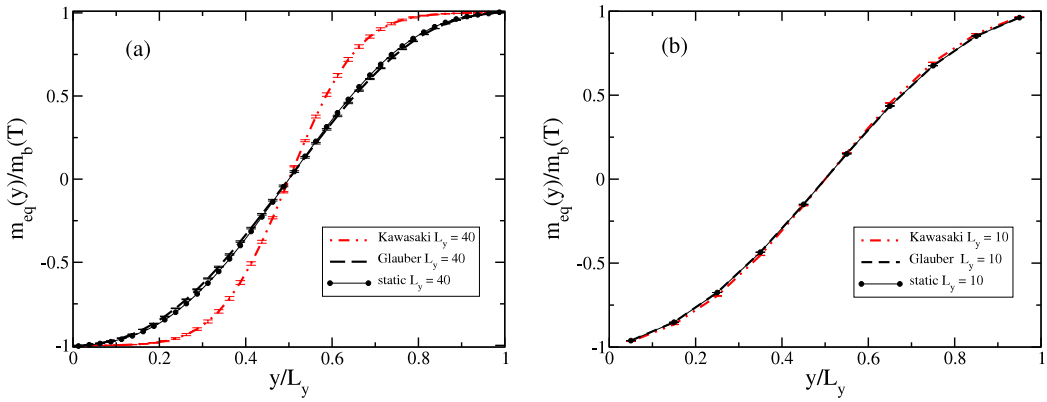

Figure 3. Magnetization profiles obtained from simulations with Kawasaki and with Glauber dynamics for $T/T_c = 0.75$, $L_x = 200$, compared with the static ones obtained by using the exact diagonalization of the transfer matrix for infinite strips $L_x = \infty$ and for two different widths (a) $L_y = 40$ and (b) $L_y = 10$.

the walls up to near the centre of the system, where the peak is now strong—see figure 2(b). In both models, the increased order near the walls and the taller, narrower peak in $E(y)$ under drive indicate that the interface is more strongly localized at the centre of the system. It is thus plausible that, as we propose and develop quantitatively in [31], that drive acts as an effective increase in confinement (i.e. a decrease in L_y) in these models. Finally we note that there are also differences between $E_x(y)$ and $E_y(y)$ in equilibrium—$E_x(y)$ is more negative than $E_y(y)$, the difference being most pronounced at the centre of the system, reflecting the fact that the interface is oriented along x.

3.2. Differences between Glauber and Kawasaki dynamics in equilibrium

We next turn to the differences between Kawasaki and Glauber dynamics for *equilibrium* systems. As noted above, in the driven case one requires particle motion rather than creation and annihilation, rendering spin-flip dynamics, such as Glauber, inappropriate. However, in an equilibrium system, any dynamics satisfying detailed balance and ergodicity must give the same averages over the time evolution *in the thermodynamic limit*. In a finite system, however, the two types of dynamics are not equivalent due to the constraint of conserved magnetization in the Kawasaki case. This is especially striking in a confined geometry such as the one we have studied in the driven case [31]—that is, in strips. Here the interface as a whole may 'wander' between the two walls under the non-conserving dynamics, since a majority of either spin species is permitted. Under conservative dynamics, such overall movement of the interface cannot occur.

For both types of dynamics we have performed a systematic study of the finite-size effects on the magnetization profile and on the two-point correlation functions. A selection of results for the magnetization profile is shown in figure 3 where $L_x = 200$ is fixed and L_y is varied, and in figure 4 where $L_y = 20$ is fixed and L_x is varied. As a benchmark we compare to results from the exact diagonalization of the transfer matrix for an infinite strip, $L_y = \text{const}$ and $L_x = \infty$.

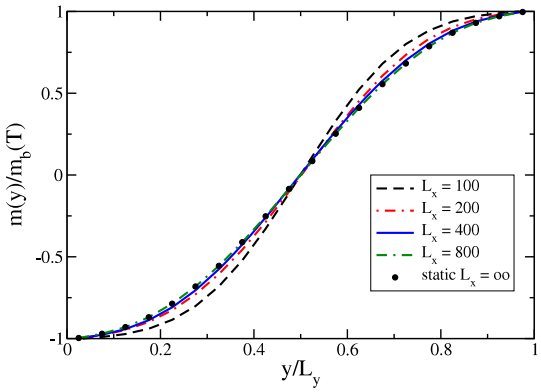

Figure 4. Magnetization profiles obtained with Kawasaki dynamics for $T/T_c = 0.75$, $L_y = 20$ and several different values of L_x (as indicated). The simulation results become indistinguishable from the static ones for an infinite strip within error bars at $L_x = 800$.

For such a system the different types of dynamics yield (time) averages for static quantities that are identical to the ensemble average. In the finite systems, we find that the non-equivalence of the two types of dynamics manifests itself more strongly for low temperatures, where the shape of the magnetization profile for non-conserved (Glauber) dynamics is affected by the local position of the interface exploring the full region of the strip. This wandering gives rise to a profile which varies linearly with position across almost the entire strip. The constraint imposed on the total magnetization in the Kawasaki dynamics prohibits this free wandering. In addition, long-wavelength fluctuations, which also smear out the interface, are cut off because L_x is finite. Short-wavelength fluctuations of large amplitude come at a large energy cost due to surface tension. As a result the profiles from Kawasaki dynamics have much larger flat regions near the walls and a far sharper interfacial region with the linear part of the profile considerably reduced as compared to the profiles obtained by Glauber dynamics. We find that with decreasing the scaling variable $L_y/\xi \sim L_y t^{\nu}$ at fixed L_x, where $t = (T - T_c)/T_c$, and $\nu = 1$ is the critical exponent for the bulk correlation length ξ, the shape of the profiles becomes more similar to the profiles from Glauber dynamics. For

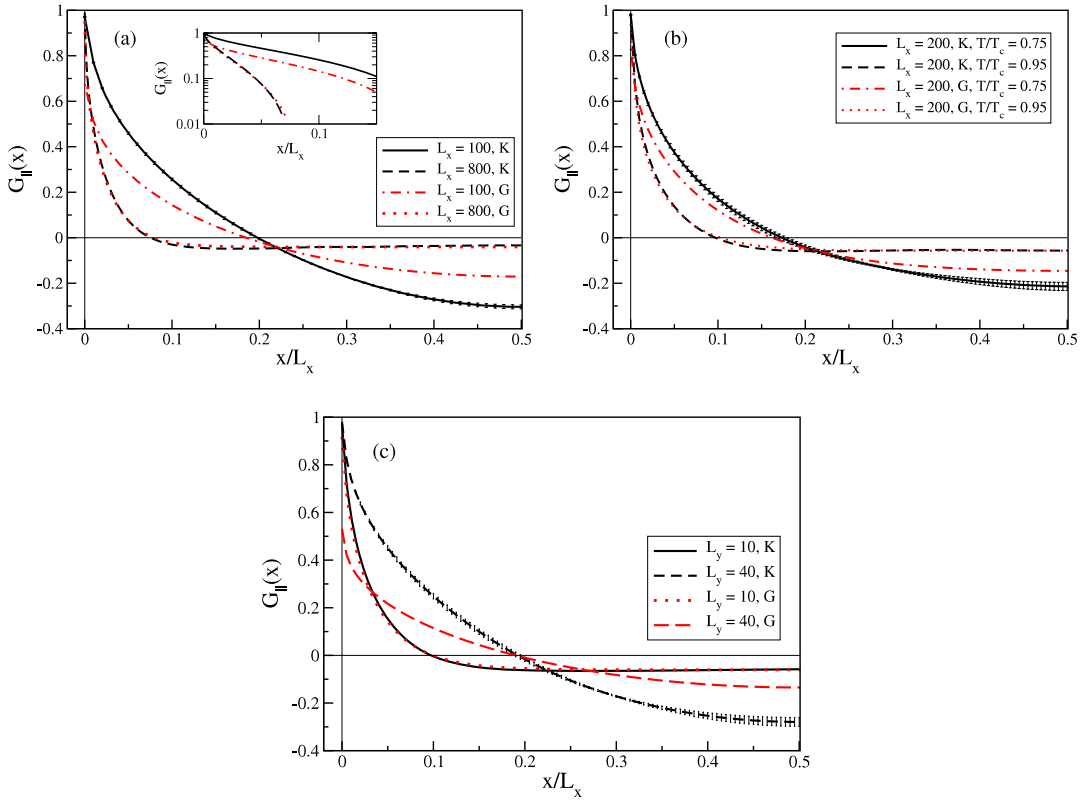

Figure 5. Comparison of the spin–spin correlation function $G_{\parallel}(x)$ as a function of scaled coordinate x/L_x, obtained by using Kawasaki and Glauber dynamics, with various lattice sizes and temperatures. Sample error bars are shown on the solid black lines. (a) Fixed $L_y = 20$ and $T/T_c = 0.75$, with varying L_x. Inset: log-linear plot for small x, showing the region of exponential-like decay for both dynamics. (b) Fixed $L_x = 200$, $L_y = 20$, with two different temperatures. (c) Fixed $L_x = 200$ and $T/T_c = 0.75$ with different values of L_y.

example, at $T/T_c = 0.75$ the Kawasaki dynamics for $L_y = 10$ give a magnetization profile which almost coincides with the one from Glauber dynamics; the latter being identical to the static result for the infinite strip (see figure 3(b)), whereas for $L_y = 40$ the differences in the shape of magnetization profiles are very pronounced (see figure 3(a)). It is also interesting to note that effects on the magnetization profiles due to L_x being finite are rather strong (see figure 4). For $L_y = 20$ at $T/T_c = 0.75$ one has to consider strips as long as $L_x = 800$ to find an agreement with the static results for infinite strips! On the one hand this might not seem surprising because of the very large lateral correlation length; for infinite strips $\xi_{\parallel} \sim L_y^2$ in two dimensions [45]. On the other hand, for Glauber dynamics the limit of the infinite strip at the same temperature and the same width of the strip is already achieved for $L_x = 200$ (not shown).

As we demonstrate in the following, the differences between results from Glauber and from Kawasaki dynamics are even more pronounced on the level of two-body functions. Due to the lack of exact results for infinite strips we are not able to judge the importance of finite-size effects associated with the finite size in the x-direction in the simulated systems. We have investigated the spin–spin pair correlation function $G(x, y, y') = \langle \sigma_i \sigma_j \rangle$, where $i = (0, y)$ and $j = (x, y')$, in particular focusing on the behaviour at the centre of the system, $G_{\parallel}(x) \equiv G(x, L_y/2, L_y/2)$; this should reveal most clearly interface-mediated correlations between pairs of spins. We have studied three different temperatures $T/T_c = 0.75, 0.85$ and 0.95, and several values of L_x and L_y, ranging from 100 to 800 and from 10 to 40, respectively. Representative results are shown in figures 5. The striking feature of these correlation functions is that they cross zero at some $x = x_0$ and saturate at a negative value $G_{\parallel}^{\mathrm{sat}}$ for larger values of x. Both x_0 and $G_{\parallel}^{\mathrm{sat}}$ depend on the temperature and on the size of the strip. At fixed L_x and T, a wider (larger value of L_y) strip gives a larger value of x_0 and a more negative saturation value. At fixed L_y and T, a longer (greater L_x) strip gives a smaller x_0 and a less negative saturation value. At fixed L_x and L_y, the higher the temperature, the smaller x_0 and the less negative $G_{\parallel}^{\mathrm{sat}}$. We associate these negative correlations with the finite-size effects causing the long contour (i.e., the path that separates two regions that are oppositely magnetized) to cross the line $y = L_y/2$ on average near $x = x_0$. Finite-size effects strongly influence the functional form of $G_{\parallel}(x)$. The exponential decay with characteristic length $\xi_{\parallel}$ expected for large x in the limit $L_x \to \infty$ and large L_y can be identified only for a rather narrow interval of intermediate values of x (see the inset of figure 5(a)).

As can be seen in figure 5(a), for short strips with $L_x = 100$ and width $L_y = 20$, the differences in correlation functions $G_{\parallel}(x)$ obtained from the different dynamics are quite pronounced. The amplitude of $G_{\parallel}(x)$ obtained by using Glauber dynamics is suppressed with respect to the one from Kawasaki dynamics, but the decay length seems to be the same

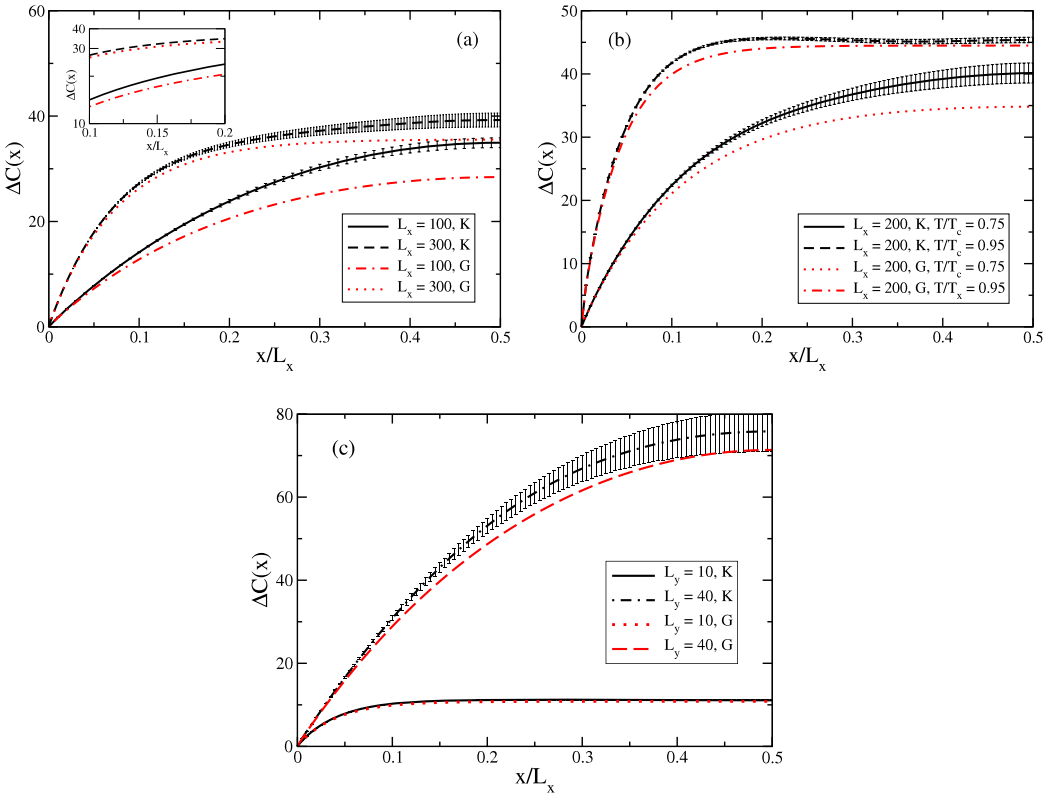

Figure 6. Comparison of the difference height–height correlation function $\Delta C(x)$ as a function of scaled coordinate x/L_x, obtained by using Kawasaki and Glauber dynamics, with various lattice sizes and temperatures. (a) Fixed $L_y = 20$ and $T/T_c = 0.75$, with varying L_x. Inset: log-linear plot for intermediate x, showing exponential-like behaviour for both dynamics. (b) Fixed $L_x = 200$, $L_y = 20$, with two different temperatures. (c) Fixed $L_x = 200$ and $T/T_c = 0.75$ with different values of L_y.

(see the inset of figure 5(a)). However, Kawasaki dynamics give rise to much more negative values of $G_{\parallel}^{\rm sat}$. Consistently with the behaviour of the magnetization profiles, $G_{\parallel}(x)$ from the two types of dynamics becomes identical only for very long strips ($L_x = 800$). Moreover, we observe that the differences in $G_{\parallel}(x)$ at fixed L_x and L_y vanish sufficiently close to T_c, where the interface becomes more diffusive and interfacial fluctuations become less important relative to bulk fluctuations. Indeed for both dynamics $G_{\parallel}(x)$ decays faster at higher temperatures, and gives the same results for a system with $L_x = 200$, $L_y = 20$—see figure 5(b). Finally, in figure 5(c) we compare the results obtained for $L_x = 200$, $T/T_c = 0.75$ and two different widths, $L_y = 10$ and 40. For narrow strips both dynamics lead to practically identical behaviour of the spin–spin correlation functions at the interface. For wider strips, which allow more wandering of the interface, the shapes of $G_{\parallel}$ differ substantially, but in a way similar to the case of fixed L_y but small L_x (compare figure 5(a)). This is because $\xi_{\parallel} \sim L_y^2$ for sufficiently large systems, so that increasing L_y at fixed L_x leads to similar finite-size effects on $\xi_{\parallel}$ as decreasing L_x at finite L_y.

We have also performed a coarse-graining procedure to study interfacial properties in terms of the (difference) height–height correlation function $\Delta C(x) = C(0) - C(x) = \frac{1}{2}\langle[h(x) - h(0)]^2\rangle$ of the local position of the interface $h(x)$ with $C(x) = \langle h(0)h(x)\rangle$. To define $h(x)$ we adopt the method of [46] and for each column evaluate the sum

$$v(h) = \sum_{y=1}^{L_y} \left[\sigma(x, y) - \Theta(y - h)\right]^2, \qquad (8)$$

$$\Theta(\zeta) = \pm 1 \qquad \text{for } \zeta \gtrless 0.$$

The value of h which minimizes the above sum defines the position of the interface in this column x.

Results obtained by using Glauber and Kawasaki dynamics are compared in figure 6 for selected values of parameters. These were obtained using single-spin code, which yields larger statistical uncertainties than the multi-spin code used in the calculation of $G_{\parallel}(x)$ above. The qualitative behaviour of the height–height correlation functions is the same for both dynamics; $\Delta C(x)$ increases sharply for short distances x and then saturates at some value $\Delta C_{\rm sat}$ which, similarly to $G_{\parallel}^{\rm sat}$, depends on the temperature and on the size of the lattice. For intermediate distances the behaviour of the difference height–height correlation function seems to be exponential in x (see inset in figure 6(a)). The main trends in differences in $\Delta C(x)$ obtained by using the two dynamics are similar to those described above for the spin–spin correlation function. They are more pronounced for small-L_x lattices—see figure 6(a), for lower temperatures—see figure 6(b), and for larger L_y lattices—see figure 6(c).

In summary, as one might expect, the significant differences between one- and two-body correlation functions

obtained by using Glauber and Kawasaki dynamics occur for values of the relevant length scales in the system L_x and L_y for which the finite-size effects for interfaces are particularly strong. At fixed temperature this takes place for the large ratio L_y^2/L_x. On the other hand increasing temperature at fixed lattice size leads to the decrease of differences.

4. Conclusions and outlook

We have presented results for the energy bond profile of a phase-separated 2d Ising model under shear-like drive. These indicate an increased localization of the interface and stronger order near the walls, providing further evidence that shear acts as effective confinement [31] in this system. The effect of boundary drive (model I) on the energy profile is quite large compared to the effect on the magnetization profile reported in [31]. This may be due to the two-body (nearest-neighbour) nature of the energy profile, whereas the magnetization is of one-body type; changes induced on the average value of a particular spin produce an amplified change in the interaction with its (also changed) neighbour.

We have also investigated the effect of using different types of dynamics in simulations of finite equilibrium systems, by measuring magnetization profiles and two-body correlation functions using both Kawasaki dynamics, which conserve magnetization, and non-conserving (Glauber) dynamics. For the magnetization profile, a longer distance L_y between the walls produces greater differences, owing to larger finite-size effects resulting from an increased lateral (interfacial) correlation length $\xi_\parallel \sim L_y^2$. This effect is also apparent for fixed L_y and varying L_x; long systems are required to make L_x large enough compared to $\xi_\parallel$ to obtain good agreement with results from Glauber dynamics, and exact transfer-matrix results. The two-body correlation functions show the same trends with varying system dimensions; for the spin–spin correlation function $G_\parallel(x)$, two important characteristics are the location x_0 at which the function crosses the x axis, and the negative saturation value $G_\parallel^{\mathrm{sat}}$ at large x. For parameters where Kawasaki and Glauber results differ, the saturation value is more negative for Kawasaki dynamics, again indicating stronger finite-size effects. This is also reflected in the difference height–height correlation function $\Delta C(x)$, which exhibits larger saturation values with Kawasaki dynamics (greater than C(0)); these correspond to a more negative $C(x)$. In conclusion, magnetization-conserving Kawasaki dynamics can give quite different results for static (not only dynamic) quantities as compared to non-conserving spin-flip dynamics, due to strong finite-size effects. The differences depend strongly on system aspect ratio as well as on temperature, since these parameters control the size of the relevant length scale, the lateral correlation length $\xi_\parallel$, relative to the system size.

The sheared Ising lattice gas provides intriguing future possibilities for investigation of steady state interfacial phenomena. On the static side, we have found evidence for scaling behaviour of the driven interfacial width and magnetization profile, condensing dependence on temperature, system size, and field gradient ω into a scaling variable. Varying the form of the driving field, e.g. considering a spatially constant field (KLS model) in confined geometry, would also be useful, in order to determine which features of the drive are important in various phenomena. We are also studying the three-dimensional generalization of our models, where the physics may be rather different. Finally, we hope that studying dynamics will reveal interesting new phenomena and provide insight into how a driving field fundamentally affects the interface.

Acknowledgments

We thank DGAL Aarts, T Bickel, D Derks, J Eggers, RML Evans, R Evans, A Gambassi, I Rehberg, B Schmittmann, and R Zia for useful discussions and the EPSRC for financial support.

References

[1] Hohenberg P C and Halperin B I 1977 *Rev. Mod. Phys.* **49** 435
[2] Bray A 1994 *Adv. Phys.* **43** 357
[3] Abraham D B, Cuerno R and Moro E 2002 *Phys. Rev. Lett.* **88** 206101
[4] Krzakała F 2005 *Phys. Rev. Lett.* **94** 077204
[5] Penrose O 1970 *Foundations of Statistical Mechanics* (Oxford: Pergamon)
[6] Glauber R 1963 *J. Math. Phys.* **4** 294
[7] Kawasaki K 1966 *Phys. Rev.* **145** 224
[8] Schmittmann B and Zia R K P 1995 *Statistical Mechanics of Driven Diffusive Systems* (*Phase Transitions and Critical Phenomena* vol 17) ed C Domb and J Lebowitz (London: Academic)
[9] Schuetz G M 2000 *Exactly Solvable Models for Many-Body Systems Far From Equilibrium* (*Phase Transitions and Critical Phenomena* vol 19) ed C Domb and J Lebowitz (London: Academic) p 1
[10] Katz S, Lebowitz J L and Spohn H 1984 *J. Stat. Phys.* **34** 497
[11] Marro J and Dickman R 1999 *Nonequilibrium Statistical Mechanics of Lattice Models* (Cambridge: Cambridge University Press)
[12] Abraham D B 1986 *Structure and Phase Transitions in Surfaces* (*Phase Transition and Critical Phenomena* vol 10) ed C Domb and J Lebowitz (London: Academic) and references therein
[13] Jasnow D 1984 *Rep. Prog. Phys.* **47** 1059 and references therein
[14] Cahn J W and Hilliard J E 1958 *J. Chem. Phys.* **28** 258
[15] Rowlinson J S and Widom B 1991 *Molecular Theory of Capillarity* (Oxford: Oxford University Press)
[16] Abraham D B and Reed P 1974 *Phys. Rev. Lett.* **43** 377
[17] Fisk S and Widom B 1969 *J. Chem. Phys.* **50** 3219
[18] Buff F P, Lovett R A and Stillinger F H 1965 *Phys. Rev. Lett.* **15** 621
[19] Maciołek A, Stecki J and Olaussen K 1994 *Phys. Rev.* B **49** 1092
[20] Abraham D B, Mustonen V and Wood A J 2004 *Phys. Rev. Lett.* **93** 076101
Abraham D B, Mustonen V and Wood A J 2004 *Phys. Rev.* E **70** 066138
[21] Bricmont J, El Mellouki A and Frohlich J 1986 *J. Stat. Phys.* **42** 743
[22] Leung K-t 1988 *J. Stat. Phys.* **50** 405
[23] Leung K-t, Mon K K, Vallés J L and Zia R K P 1988 *Phys. Rev. Lett.* **61** 1744
Leung K-t, Mon K K, Vallés J L and Zia R K P 1989 *Phys. Rev.* B **39** 9312
[24] Leung K-t and Zia R K P 1993 *J. Phys. A: Math. Gen.* **26** L737
[25] Zia R K P and Leung K-t 1991 *J. Phys. A: Math. Gen.* **24** L1399

[26] Derks D, Aarts D G A L, Bonn D, Lekkerkerker H N W and Imhof A 2006 *Phys. Rev. Lett.* **97** 038301
[27] Aarts D G A L, Schmidt M and Lekkerkerker H N W 2004 *Science* **304** 847
[28] Derks D, Wisman H, von Blaaderen A and Imhof A 2004 *J. Phys.: Condens. Matter* **16** S3917
[29] Lettinga M P, Wang H and Dhont J K G 2004 *Phys. Rev.* E **70** 061405
[30] Bedeaux D and Weeks J D 1985 *J. Chem. Phys.* **82** 972
Weeks J D 1984 *Phys. Rev. Lett.* **52** 2160
[31] Smith T H R, Vasilyev O, Abraham D B, Maciołek A and Schmidt M 2008 *Phys. Rev. Lett.* **101** 067203
[32] Stecki J and Dudowicz J 1985 *Proc. R. Soc. Lond.* A **400** 263
[33] Padilla P, Toxvaerd S and Stecki J 1995 *J. Chem. Phys.* **103** 716
[34] Germano G and Schmid F 2005 *J. Chem. Phys.* **123** 214703
[35] Sahai M K and Sengupta S 2008 *Phys. Rev.* E **77** 032601
[36] Cirillo E N M, Gonnella G and Saracco G P 2005 *Phys. Rev.* E **72** 026139
[37] Allen R J, Valeriani C, Tanase-Nicol S, ten Wolde P R and Frenkel D 2008 arXiv:0802.3811
[38] Henrich O *et al* 2007 *J. Phys.: Condens. Matter* **19** 205132
Brader J M *et al* 2007 *Phys. Rev. Lett.* **98** 058301
Lettinga M P *et al* 2004 *Phys. Rev.* E **70** 061405
[39] Onuki A 1997 *J. Phys.: Condens. Matter* **9** 6119
[40] Potiguar F Q and Dickman R 2006 *Braz. J. Phys.* **36** 736
Potiguar F Q and Dickman R 2006 *Eur. Phys. J.* B **52** 83
[41] Newman M E J and Barkema G T 1999 *Monte Carlo Methods in Statistical Physics* (Oxford: Oxford University Press)
[42] Rikvold P A and Kolesik M 2002 *J. Phys. A: Math. Gen.* **35** L117
[43] Rikvold P A and Kolesik M 2003 *Phys. Rev.* E **67** 066113
[44] van Gemmert S, Barkema G T and Puri S 2005 *Phys. Rev.* E **72** 046131
[45] Maciołek A and Stecki J 1996 *Phys. Rev.* B **54** 1128
[46] De Virgiliis A, Albano E V, Müller M and Binder K 2005 *Physica* A **352** 477